Journal of Molecular Cell Biology (2023), 15(3), mjad017 https://doi.org/10.1093/jmcb/mjad017
Published online March 15, 2023

Article

TMPRSS2 and SARS-CoV-2 SPIKE interaction assay for uHTS

Danielle Cicka[1,2,†], Qiankun Niu[1,†], Min Qui[1,3], Kun Qian[1], Eric Miller[1,4], Dacheng Fan[1], Xiulei Mo[1,4], Andrey A. Ivanov[1,3,4], Stefan G. Sarafianos[5], Yuhong Du[1,3,4], and Haian Fu[1,3,4,*]

[1] Department of Pharmacology and Chemical Biology, Emory University School of Medicine, Atlanta, GA 30322, USA
[2] Graduate Program in Molecular and Systems Pharmacology, Laney Graduate School of Emory University, Atlanta, GA 30322, USA
[3] Emory Chemical Biology Discovery Center, Emory University School of Medicine, Atlanta, GA 30322, USA
[4] Winship Cancer Institute of Emory University, Atlanta, GA 30322, USA
[5] Laboratory of Biochemical Pharmacology, Department of Pediatrics, Emory University School of Medicine, Atlanta, GA 30322, USA
[†] These authors contributed equally to this work.
* Correspondence to: Haian Fu, E-mail: hfu@emory.edu

Edited by Jiarui Wu

SARS-CoV-2, the coronavirus that causes the disease COVID-19, has claimed millions of lives over the past 2 years. This demands rapid development of effective therapeutic agents that target various phases of the viral replication cycle. The interaction between host transmembrane serine protease 2 (TMPRSS2) and viral SPIKE protein is an important initial step in SARS-CoV-2 infection, offering an opportunity for therapeutic development of viral entry inhibitors. Here, we report the development of a time-resolved fluorescence/Förster resonance energy transfer (TR-FRET) assay for monitoring the TMPRSS2–SPIKE interaction in lysate from cells co-expressing these proteins. The assay was configured in a 384-well-plate format for high-throughput screening with robust assay performance. To enable large-scale compound screening, we further miniaturized the assay into 1536-well ultrahigh-throughput screening (uHTS) format. A pilot screen demonstrated the utilization of the assay for uHTS. Our optimized TR-FRET uHTS assay provides an enabling platform for expanded screening campaigns to discover new classes of small-molecule inhibitors that target the SPIKE and TMPRSS2 protein–protein interaction.

Keywords: SARS-CoV-2, COVID-19, protein–protein interaction, TMPRSS2, SPIKE, high-throughput screening, TR-FRET

Introduction

The coronavirus disease 2019 (COVID-19), caused by the infection of severe acute respiratory syndrome coronavirus 2 (SARS-CoV-2), has become a global pandemic with >6 million deaths by early January 2023 (https://www.worldometers.info/coronavirus/). The nonspecific symptoms of cough, fever, malaise, and fatigue make early detection difficult (https://www.cdc.gov/coronavirus/2019-ncov/symptoms-testing/symptoms.html). While mortality rates have been challenging to calculate as well, progression to acute respiratory distress syndrome may lead to survival rates as low as 25% (Yang et al., 2020). Although vaccination broadly provides effective protection against viral infection, benefits of vaccination are prophylactic by design. In contrast, small-molecule therapeutics that target viral propagation mechanisms are able to combat viral replication after infection. However, small-molecule antiviral agents that effectively treat SARS-CoV-2 infection have just begun to reach the market (Gupta et al., 2022; Hammond et al., 2022; Jayk Bernal et al., 2022). Because viral resistance to the few existing monotherapeutic options is virtually inevitable, additional therapies, and novel combinations thereof, are critically needed to increase survival rates of severe COVID-19 patients and stay one step ahead of this dynamic, devastating virus amidst this persisting global pandemic.

Since early on in the pandemic, the multi-step process of viral entry has been implicated as a promising therapeutic target for SARS-CoV-2 and has been the primary focus of vaccine development (Malik et al., 2021). SARS-CoV-2 infects host cells through two main pathways, each of which relies on the high-affinity interaction between the SARS-CoV-2 glycoprotein SPIKE and the host angiotensin-converting enzyme 2 (ACE2) receptor. The SPIKE protein itself is a heavily glycosylated trimer with each

Received April 28, 2022. Revised November 21, 2022. Accepted March 13, 2023.

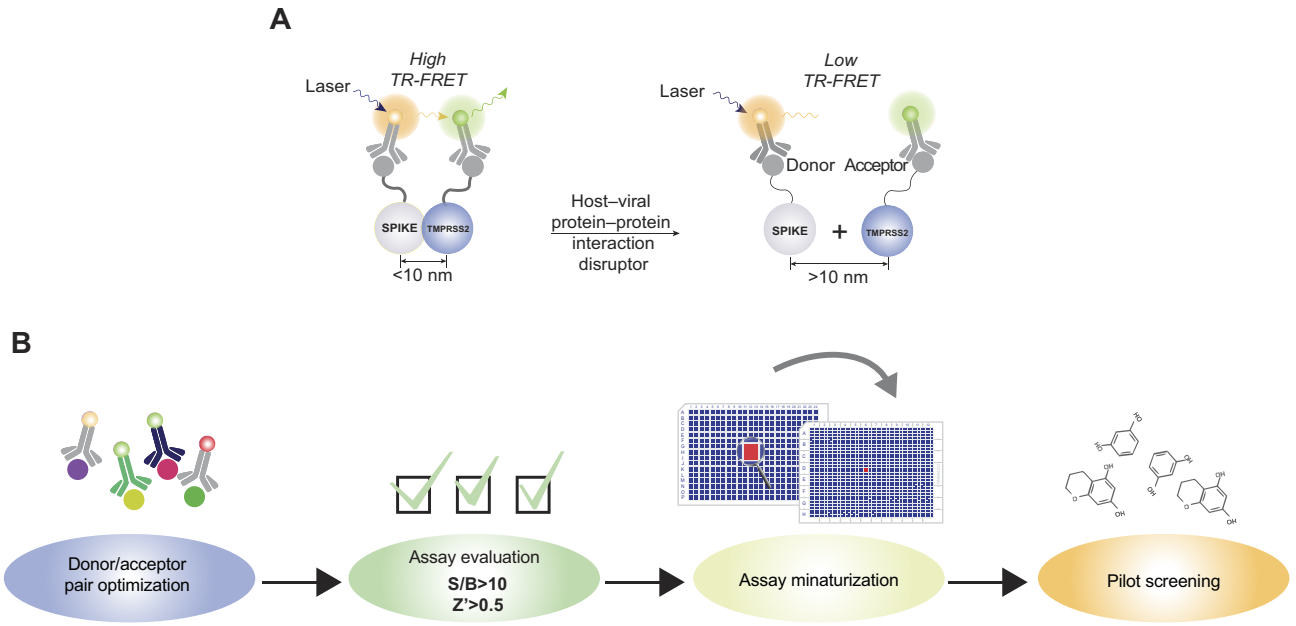

Figure 1 TMPRSS2–SPIKE TR-FRET interaction assay and workflow. (**A**) TR-FRET model. SPIKE and TMPRSS2 are fused to tags that interact with antibodies conjugated to fluorophores. When the proteins are in close proximity (<10 nm), excitation of a donor fluorophore can cause excitation of the acceptor fluorophore. (**B**) Workflow of TR-FRET assay development and screening. Expression of various TMPRSS2 and SPIKE proteins and different tags were tested with different donor and acceptor combinations in TR-FRET. For the pair chosen, assay evaluation for HTS and miniaturization were done followed by a small-scale pilot screen of bioactive compounds.

monomer containing a receptor-binding domain. One of the viral entry pathways involves pre-activation of the receptor-binding domain by a proprotein convertase, such as furin, which renders SPIKE accessible for binding to the ACE2 receptor. In contrast, the direct fusion pathway begins after binding to the ACE2 receptor when the SPIKE protein is cleaved by transmembrane serine protease 2 (TMPRSS2), which exposes the S2 subunit for initiation of viral fusion to the cell membrane (Jackson et al., 2022).

While cleavage by furin increases efficiency of viral fusion, it is not essential (Papa et al., 2021). However, cleavage by TMPRSS2 is critical for viral fusion in cells in which TMPRSS2 is present. In fact, inhibition of TMPRSS2 activity has been shown to reduce SARS-CoV-2 entry *in vitro* (Hoffmann et al., 2020, 2021). Even so, no chemical inhibitors of the SARS-CoV-2 TMPRSS2–SPIKE interaction, to our knowledge, have yet been identified.

Despite the development of vaccines, newly diagnosed cases and deaths continue to increase around the world. As a consequence, it is urgent that new and improved treatment options are rapidly developed and clinically deployed. In this study, we report the development of an ultrahigh-throughput screening (uHTS) assay that enables the discovery of small-molecule protein–protein interaction (PPI) disruptors of the TMPRSS2–SPIKE interaction (Figure 1A). The assay developed herein utilizes the homogenous time-resolved fluorescence/Förster resonance energy transfer (TR-FRET) format to monitor the interactions in cell lysates without the need for purification of the interaction partners (Klostermeier and Millar, 2002; Xiong et al., 2018). Extensive optimization of the assay conditions led to robust assay performance with a high signal-to-background (S/B) ratio, thereby rendering it suitable for efficient and sensitive SARS-CoV-2 entry inhibitor discovery.

As a proof of concept, we screened for inhibitors targeting the TMPRSS2–SPIKE interaction using bioactive chemical libraries that contain approved drugs, as well as investigational drugs (Figure 1B). Utilizing drugs that are already FDA-approved or currently under clinical investigation can expedite the drug development process, providing the potential for rapid translation from laboratory results to patient bedside.

This optimized TMPRSS2–SPIKE interaction assay provides a platform for future expanded screenings. Identified TMPRSS2–SPIKE interaction inhibitors may provide critical insights into the viral entry mechanisms and lead to the development of effective therapeutic agents against COVID-19.

Results

Expression of SPIKE and TMPRSS2 proteins

To probe the molecular interaction of TMPRSS2 and SPIKE at the host–virus interface, genes encoding SPIKE and TMPRSS2 were cloned into expression vectors suitable for expressing the respective proteins. These expressed proteins could then be used in assays to monitor PPIs using TR-FRET and affinity chromatography techniques. To enable the coupling of fluorophores and affinity resins, both SPIKE and TMPRSS2 proteins were fused

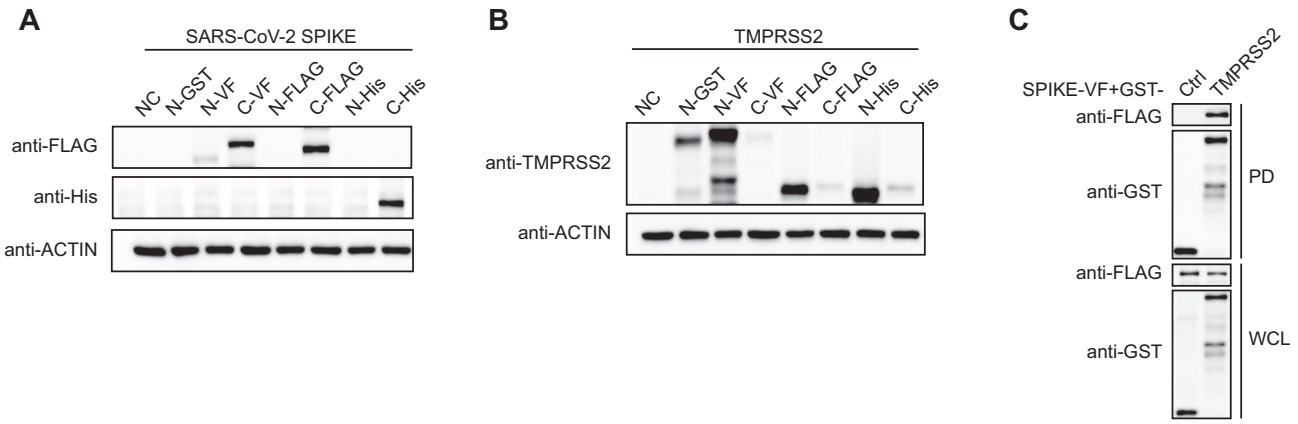

Figure 2 Expression of TMPRSS2 and SPIKE constructs and confirmation of binding in HEK-293T cells. (**A**) Expression of SPIKE constructs determined by western blotting. C-terminal tagged SPIKE expressed well and was therefore selected for this study. No expression of N-GST was detected (data not shown). NC, no construct; N, N-terminal tag; C, C-terminal tag. (**B**) Expression of TMPRSS2 constructs determined by western blotting. N-terminal tagged TMPRSS2 expressed well and was therefore selected for this study. (**C**) GST pulldown (PD) results of SPIKE-VF and GST-TMPRSS2 overexpressed in HEK-293T cells. PD and whole-cell lysate (WCL) samples were subjected to western blotting as indicated.

with various epitope tags, including glutathione-S-transferase (GST), 6× histidines (His), FLAG, and Venus-FLAG (VF). To test the potential configuration effect of tags for expression or coupling, we also generated SPIKE and TMPRSS2 proteins with tags at either the N-terminal or C-terminal end. A panel of plasmids that express SPIKE or TMPRSS2 proteins with N-terminal fusion of GST, VF, FLAG, and His tags and C-terminal fusion of VF, FLAG, and His tags were tested in HEK-293T cells. The expressed proteins were monitored by western blotting with respective antibodies against a specific tag or protein (Figure 2A and B). As shown, C-terminal fusions of SPIKE expressed well, while N-terminal fusions did not (Figure 2A). Conversely, N-terminal fusions of TMPRSS2 expressed well, while C-terminal fusions did not (Figure 2B).

Confirmation of PPI in HEK-293T cells with affinity chromatography assays

SPIKE and TMPRSS2 have been found to interact with each other, as the cleavage of SPIKE by TMPRSS2 was previously reported (Hoffmann et al., 2020, 2021). To verify this PPI for our assay design, we determined whether the interactions could be detected in the HEK-293T mammalian system. For this purpose, we utilized the affinity GST pulldown assay. Glutathione Sepharose was used to precipitate GST-tagged TMPRSS2. After washing, the presence of SPIKE-VF in the GST-TMPRSS2 complex was detected by western blotting with an anti-FLAG antibody. As shown in Figure 2C, SPIKE-VF was found in the GST-TMPRSS2 complex, supporting the association of TMPRSS2 and SPIKE in HEK-293T cells. These co-expressed interaction partners could then be used for high-throughput screening (HTS) assays.

Design of TR-FRET assay for monitoring TMPRSS2 and SARS-CoV-2 SPIKE interaction

To identify TMPRSS2 and SPIKE interaction inhibitors, we developed a proximity-based TR-FRET assay to monitor the association of His-TMPRSS2 and SPIKE-FLAG in a mammalian system. TR-FRET relies on the principle that a protein indirectly labeled with a donor fluorophore-conjugated antibody can emit a signal that will excite an acceptor fluorophore-conjugated antibody labeling another protein if those proteins are within close proximity (<10 nm). Therefore, signal generated from the acceptor fluorophore can indicate interaction between the two proteins of interest (Figure 1A). The tags chosen for each protein and the TR-FRET antibodies can make a critical difference in optimizing the signal for TR-FRET detection of the PPI. The affinity tags of the proteins can interfere with the orientation of the PPI and the configuration of TR-FRET antibodies.

The TMPRSS2 and SPIKE TR-FRET assay was configured by choosing pairs of tagged TMPRSS2 and SPIKE that allow for coupling of a donor and acceptor fluorophore pair. As described above, SPIKE-VF, SPIKE-FLAG, and SPIKE-His expressed well in HEK-293T cells. His-TMPRSS2, GST-TMPRSS2, VF-TMPRSS2, and FLAG-TMPRSS2 expressed well in HEK-293T cells. Terbium (Tb), used as the conjugated donor, was laser-excited at 337 nm causing emission at 615 nm. D2 was used as the conjugated acceptor with excitation and emission wavelengths around 615 nm and 665 nm, respectively. The TR-FRET signal can be determined by the ratio of the signal generated at 665 nm/615 nm.

The co-expressed SPIKE-VF and His-TMPRSS2 were coupled with anti-FLAG-antibody-conjugated Tb as a donor and anti-His-conjugated D2 as an acceptor. This interaction pair (combination 1) was tested in the TR-FRET assay, which gave rise to an S/B ratio of 23, suggesting the interaction of SPIKE and TMPRSS2 (Figure 3A). To test whether a different combination of tags or antibody pairs would improve the S/B, SPIKE and TMPRSS2 fusion proteins were co-expressed in various combinations such that a donor and acceptor fluorophore antibody pair was able to bind to either SPIKE and TMPRSS2 or TMPRSS2 and SPIKE, respectively. The following donor/acceptor

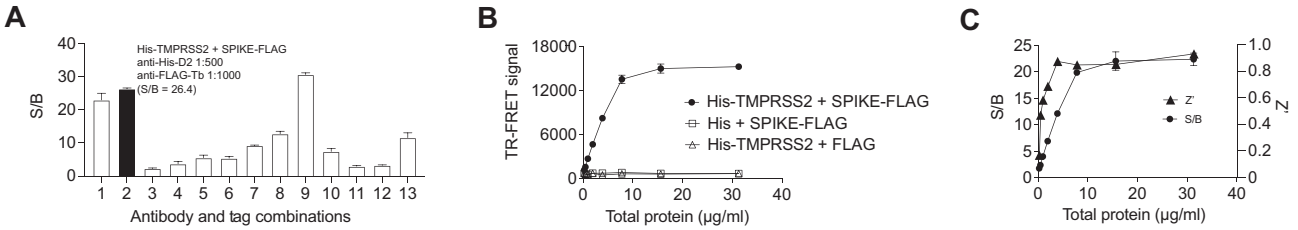

Figure 3 TMPRSS2–SPIKE TR-FRET assay development in 384-well format. (**A**) Various tags and donor/acceptor fluorophore-conjugated antibodies were used to find the optimal combination for TR-FRET. Combinations are as follows: (1) His-TMPRSS2–SPIKE-VF with FLAG-Tb/His-D2; (2) His-TMPRSS2–SPIKE-FLAG with FLAG-Tb/His-D2; (3) His-TMPRSS2–SPIKE-VF with His-Tb/FLAG-D2; (4) His-TMPRSS2–SPIKE-FLAG with His-Tb/FLAG-D2; (5) GST-TMPRSS2–SPIKE-VF with FLAG-Tb/GST-D2; (6) GST-TMPRSS2–SPIKE-FLAG with FLAG-Tb/GST-D2; (7) GST-TMPRSS2–SPIKE-VF with GST-Tb/FLAG-D2; (8) GST-TMPRSS2–SPIKE-FLAG with GST-Tb/FLAG-D2; (9) VF-TMPRSS2–SPIKE-His with FLAG-Tb/His-D2; (10) VF-TMPRSS2–SPIKE-His with His-Tb/FLAG-D2; (11) FLAG-TMPRSS2–SPIKE-His with His-Tb/FLAG-D2; (12) GST-TMPRSS2–SPIKE-His with His-Tb/GST-D2; and (13) GST-TMPRSS2–SPIKE-His with GST-Tb/His-D2. Combination 2 was chosen for further evaluation. (**B**) TR-FRET signal at 2-fold dilution of lysate from HEK-293T cells overexpressing His-TMPRSS2 and SPIKE-FLAG. Cells were lysed in 1% NP-40 lysis buffer, and cell lysate was serially diluted in FRET buffer. Error bars represent standard deviation of $n = 3$ values. (**C**) TR-FRET S/B ratio and Z-factor (Z′) at 2-fold dilution of lysate from cells overexpressing His-TMPRSS2 and SPIKE-FLAG. Circles represent S/B ratios, and triangles represent Z′ ($n = 3$). Error bars represent standard deviation of $n = 3$ values.

conjugated antibody pairs were tested in the panel of TR-FRET assays: His-Tb/FLAG-D2, FLAG-Tb/His-D2, His-Tb/GST-D2, GST-Tb/His-D2, FLAG-Tb/GST-D2, and GST-Tb/FLAG-D2. As shown in Figure 3A, S/B ratios >23 were observed for combinations 2 and 9. Combination 2 (His-TMPRSS2–SPIKE-FLAG with anti-His-D2 and anti-FLAG-Tb antibodies) was ultimately chosen for further evaluation due to the smaller protein tags that were less likely to interfere with conformation of the PPI.

Optimization of TR-FRET assay for HTS

Among various tested combinations of tags and antibodies, the combination of His-TMPRSS2–SPIKE-FLAG with anti-His-D2 and anti-FLAG-Tb antibodies was selected for further optimization for HTS. To determine the optimal cell lysate concentration that generates an HTS-compatible signal, we collected lysate from cells expressing the fusion proteins and controls, and we performed 2-fold serial dilutions in a 384-well plate to determine the TR-FRET signal at various lysate concentrations. Such lysate titration allows the determination of optimal antibody-to-protein ratios. We found that the TR-FRET signal increased in a dose-dependent manner with cell lysate concentrations of protein, which showed a large dynamic range of the assay for further assay performance evaluation at several lysate dilutions (Figure 3B).

To evaluate the performance of the assay, we used two parameters: Z-factor and S/B ratio. The Z-factor, a measure of the assay quality for HTS, was calculated for each dilution. A Z-factor >0.5 and <1 indicates a robust assay for HTS. The S/B ratio of the lysate over various dilutions was calculated to determine the lysate dilution that provided a robust assay window. At lysate concentrations of 4–32 µg/ml, a robust assay window with S/B >10 and Z-factor >0.5 was observed (Figure 3C), and the lysate concentration of 10 µg/ml was selected for further DMSO tolerance evaluation.

Next, the assay tolerance to DMSO was tested, because small molecules utilized during screening are typically dissolved in DMSO. While the S/B was maintained >20 even at 10% DMSO (Figure 4A), compounds would be tested at a DMSO concentration ≤2%. Furthermore, as compounds will be incubated with the TR-FRET lysate for at least 1 h, it is important to ensure that the TR-FRET signal is stable. Therefore, the TR-FRET assay was evaluated over time, and the signal was found to be stable up to 48 h (Figure 4B).

Miniaturization of TR-FRET assay into 1536-well uHTS format

Although optimized and evaluated in a high-throughput 384-well format, the TR-FRET assay can be still costly and time-intensive when thousands of compounds are being screened, due to the number of plates involved, the amount of lysate needed, and especially the amount of conjugated antibodies required. Therefore, reducing the quantities of required reagents and the overall amount of lysate can be greatly beneficial for large-scale screening of compounds.

The 1536-well-plate uHTS format may reduce not only the required quantity of each reagent per well but also the mass of each library compound used for the screening. However, the signal and Z-factor must be maintained in a 1536-well-plate format to ensure the uHTS assay with robust performance. Thus, we tested whether the TMPRSS2–SPIKE TR-FRET assay developed in a 384-well plate, using 30 µl of reaction buffer, could be miniaturized to a 1536-well-plate format that utilizes 5 µl of reaction buffer (Figure 5A). The same lysate was tested in 384-well and 1536-well plates side-by-side and produced a robust TR-FRET signal compared to buffer alone in both formats (Figure 5B). The Z-factors for both formats were determined to be >0.5, indicating that the 1536-well format can also be used as a sensitive assay with the desired dynamic range to monitor the interaction of TMPRSS2 and SPIKE proteins (Figure 5C).

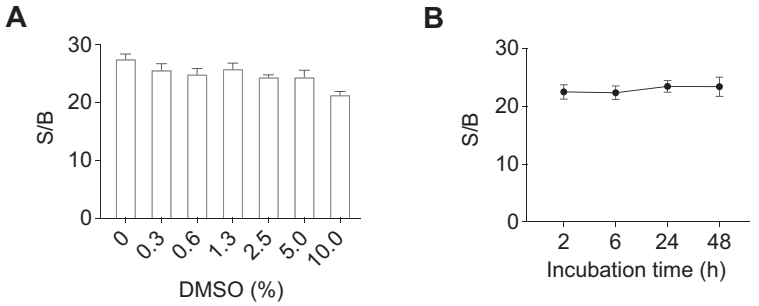

Figure 4 TMPRSS2 and SPIKE TR-FRET assay optimization in 384-well format. (**A**) Stability of TR-FRET signal in different concentrations of DMSO. Error bars represent standard deviation of $n = 3$ values. (**B**) Temporal stability of TR-FRET signal over 48 h. Error bars represent standard deviation of $n = 3$ values. TR-FRET signals were generated from cell lysate expressing His-TMPRSS2–SPIKE-FLAG with a total protein concentration at 10 μg/ml for both **A** and **B**.

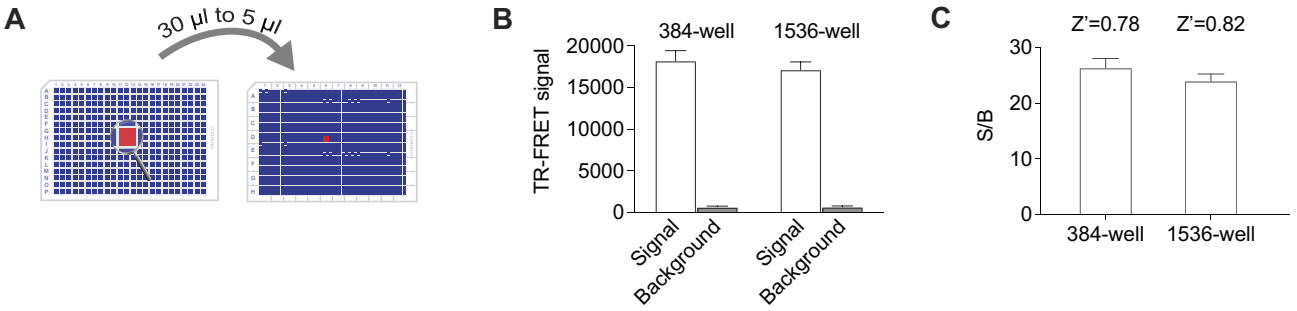

Figure 5 TR-FRET assay miniaturization for 1536-well format. (**A**) Scaling down from 384-well plates used for assay development, which uses 30 μl of TR-FRET reaction buffer per well, to 1536-well plates for uHTS, which utilizes 5 μl of TR-FRET reaction buffer. (**B**) Comparison of TR-FRET signal in 384- and 1536-well plates. TR-FRET signals were generated with same TR-FRET reaction mixture containing 10 μg/ml total protein and antibodies at working concentration (FLAG-Tb at 1:1000 and His-D2 at 1:500). Error bars represent standard deviation of $n = 5$ values. (**C**) S/B ratios and Z′ of TR-FRET assay in 384- and 1536-well-plate formats. Error bars represent standard deviation of $n = 5$ values.

Pilot screening with bioactive chemical libraries

To determine the utility of the TMPRSS2–SPIKE TR-FRET assay for uHTS, a pilot screen of the LOPAC and Emory Enriched Bioactive Library (EEBL) chemical libraries was conducted (Table 1). The LOPAC library contains 1280 pharmacologically active compounds, and the EEBL contains 2036 pharmacologically active compounds, including many FDA-approved drugs (Mo et al., 2019; Tang et al., 2021). The LOPAC library is often used for pilot screens and is well annotated. Additional inclusion of the EEBL library allowed for potential repurposing of drugs if a hit was found among these compounds.

The S/B and Z-factor were calculated for each 1536-well plate used in the screening to ensure consistency and reproducibility (Figure 6A and B). Compounds were added with a pin tool from a stock 384-well compound plate and tested in quadruplicate at a single final concentration of 20 μM. Ninety-five compounds showed <50% of the control signal, with a hit rate of 2.86% (Figure 6C).

Confirmation of top hits from pilot uHTS

After excluding fluorescence interference compounds and promiscuous compounds from 95 primary hits, 63 compounds were cherry-picked from the library stock and tested in dose–response (DR) format in the TR-FRET uHTS assay with a dose range from 0.9 to 30 μM using 2-fold serial dilutions. From DR testing, 36 compounds showed inhibition of TR-FRET signal in a dose-dependent manner. Out of the 36 compounds, 34 were available to be reordered from commercial vendors and re-tested in the TR-FRET assay with a DR range from 0.01 to 100 μM using 2-fold serial dilutions. Thirty-one of the reordered compounds had an IC_{50} <50 μM. For example, caffeic acid phenethyl ester (CAPE, $IC_{50} = 13.85$ μM), gossypol acetate ($IC_{50} = 0.69$ μM), and verteporfin ($IC_{50} = 14.74$ μM) showed dose-dependent inhibition of the TR-FRET signal (Figure 7A–C). Though favorable in TR-FRET, these compounds needed to be further evaluated in orthogonal assays for inhibition of the PPI to validate and narrow down the top hits.

Table 1 Protocol of pilot screening using TR-FRET assay.

Step	Parameter	Value	Description	Notes
1	Serial diluting lysate in a 384-well plate and adding antibodies	30 μl/well	Test TR-FRET signal with cell lysate co-expressing His-TMPRSS2 and SPIKE-FLAG, final concentration of His-D2 at 1:500 and FLAG-Tb at 1:1000	His-TMPRSS2 (1 μg) and SPIKE-FLAG (2 μg) were co-transfected in each well of a 6-well plate for 48 h. Cells were collected and lysed in 200 μl 1% NP40 buffer (20 mM Tris–HCl, 137 mM NaCl, 2 mM EDTA, 5% glycerol, and 1% NP-40) with 5 sec of sonication. Cell lysate was serially diluted with FRET buffer (20 mM Tris–HCl, pH 7.0, 50 mM NaCl, and 0.01% NP-40) for signal detection in a 384-well plate (solid-bottom, black, untreated, standard base; Corning, 3573).
2	Selecting lysate dilution fold based on FRET signal in Step 1 and preparing TR-FRET reaction mixture	5 μl/well	Dilute cell lysate (usually 5–15 μg/ml) and antibodies in FRET buffer and dispense into 1536-well plates	TR-FRET reaction mixture was dispensed into 1536-well plates (solid-bottom, black, untreated, standard base; Corning, 3724).
3	Adding compound (1 mM library stock)	0.1 μl/well	In quadruplicate	Compounds were stored at 1 mM in DMSO in 384-well plates, and 0.1 μl was added to each well in 1536-well plates using pin tool integrated with a Beckman NX.
4	Incubation	>1 h	Compounds and TR-FRET reaction incubated at 4°C	The 1536-well plates were incubated at 4°C with the top plate covered.
5	Reading TR-FRET signal	Excitation: 337 nm (laser); emission 1: 615 nm; emission 2: 665 nm	Time-resolved fluorescence	Plates were read with the BMG LABTECH PHERAstar FSX plate reader with 50 μs delay.

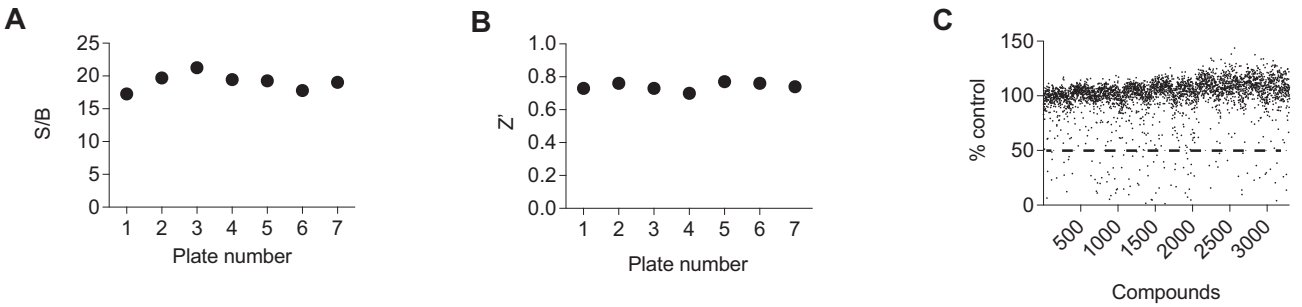

Figure 6 Pilot screening in 1536-well uHTS format. (**A**) S/B for each 1536-well plate used for pilot screening. (**B**) Z′ for each 1536-well plate used for pilot screening. (**C**) TR-FRET signal of compounds from EEBL and LOPAC libraries, expressed as percent of the control signal. Compounds with TR-FRET signal <50% of control were selected as primary hits. Screening details are found in Table 1.

Orthogonal NanoBiT assay for hit validation

NanoLuc Binary Technology (NanoBiT) allows for monitoring PPIs in a live-cell format utilizing protein-fragment complementation. The nanoluciferase protein is divided into Large BiT (LgBiT) and Small BiT (SmBiT) components that can be added as tags onto the proteins of interest (Dixon et al., 2016). Therefore, when the proteins are in close proximity, a functional nanoluciferase protein can generate a measurable signal in the presence of a substrate. The affinity of the LgBiT and SmBiT subunits is low in the basal state, thus reducing background noise. NanoBiT signals were generated by co-expressing SmBiT-TMPRSS2 and SPIKE-LgBiT (Supplementary Figure S1A–C).

In this NanoBiT assay, the top 31 compounds from TR-FRET assay were tested. Seven out of 31 showed inhibition of the signal in a dose-dependent manner. Because some of these compounds could be false positives due to luciferase interference, full-length nanoluciferase was then included as a control to exclude interference compounds that are not suitable for evaluation in this assay. Three compounds, CAPE, gossypol acetate, and verteporfin, were found to have dose-dependent inhibition in the NanoBiT assay. Each of them exhibited a dose–inhibition curve other than the nanoluciferase signal curve, suggesting specific effects on the PPI rather than the nanoluciferase signal itself (Figure 7D–F). These three compounds have been further validated, but the other top four compounds from TR-FRET, AG-490 (IC_{50} ~19 μM), closantel (IC_{50} ~17 μM), eltrombopag olamine (IC_{50} ~20 μM), and GW4064 (IC_{50} ~7 μM), require further investigation.

To support the use of this TR-FRET assay for discovering inhibitors of the TMPRSS2–SPIKE interaction, thermal shift assays were used to validate whether these seven compounds

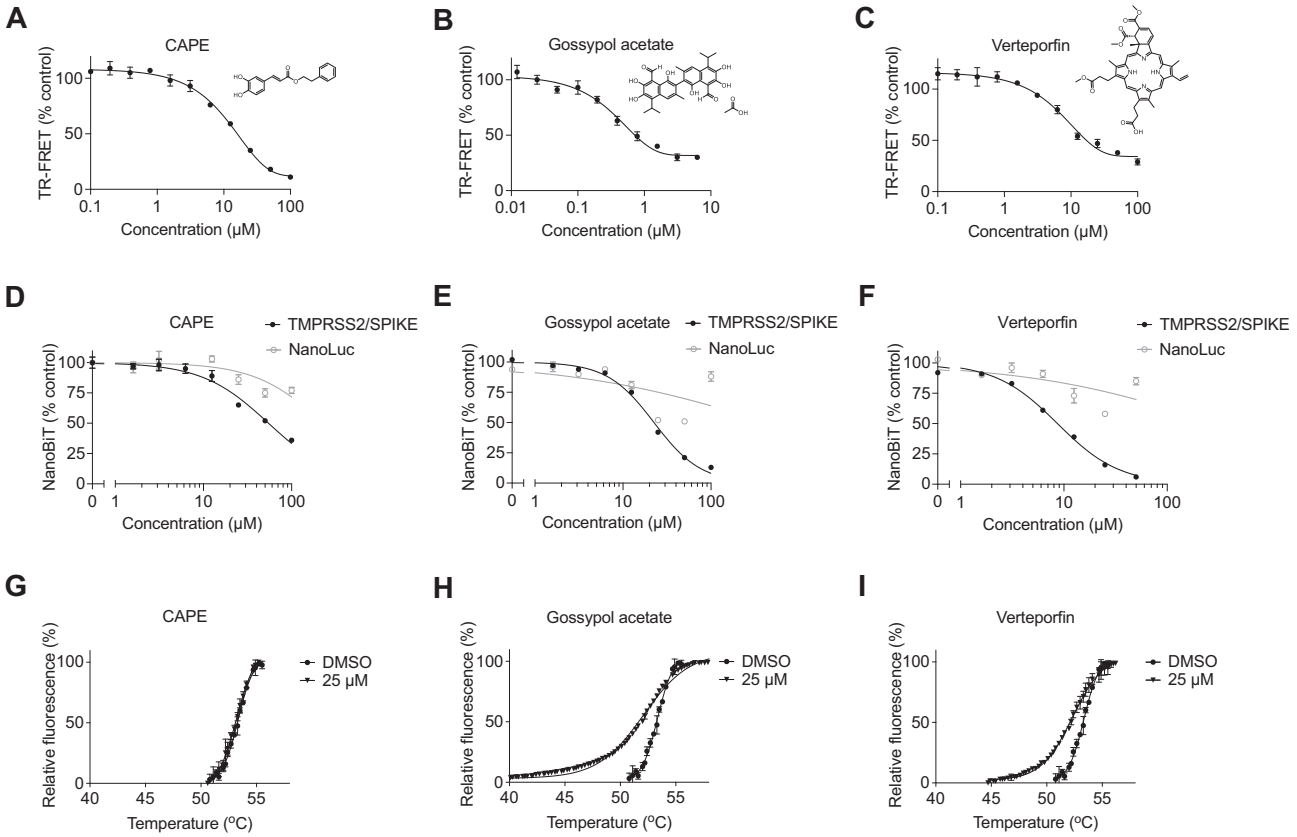

Figure 7 DR confirmation and orthogonal assay validation of reordered primary hits. (**A**–**C**) DR curves from TR-FRET assay showing the disruption of TMPRSS2–SPIKE interaction by CAPE (**A**), gossypol acetate (**B**), and verteporfin (**C**). Cell lysate expressing His-TMPRSS2 and SPIKE-FLAG was treated with compounds at a dose range from 0.01 to 100 μM. Compound structures were generated using the PyMol software. Error bars represent standard deviation of $n = 4$ values. (**D**–**F**) Dose-dependent curves from the NanoBiT assay showing the disruption of TMPRSS2–SPIKE interaction by CAPE (**D**), gossypol acetate (**E**), and verteporfin (**F**). HEK-293T cells (3500 cells/well) expressing SmBiT-TMPRSS2 and SPIKE-LgBiT were replaced into a 1536-well plate for compound treatment at a dose range from 0.01 to 100 μM. Error bars represent standard deviation of $n = 4$ values. (**G**–**I**) Thermal shift analysis of SPIKE-S2 domain with CAPE (**G**), gossypol acetate (**H**), and verteporfin (**I**). Purified His-tagged SPIKE-S2 was applied to determine the protein thermal stability by measuring fluorogenic readout from SYPRO Orange dye. Error bars represent standard deviation of $n = 2$ values.

bound to SPIKE. Two compounds, CAPE and AG-490, did not show a change in the thermal shift curve of His-SPIKE-S2 compared to the DMSO control (Figure 7G; Supplementary Table S1). In contrast, four compounds, including gossypol acetate and verteporfin, showed thermal shift of His-SPIKE-S2 (Figure 7H and I; Supplementary Table S1). GW4064 interfered with the assay and could not be evaluated.

These results indicated that gossypol acetate and verteporfin may inhibit the TMPRSS2–SPIKE interaction, as shown by TR-FRET and NanoBiT assays, through binding to SPIKE-S2 domain, as revealed by thermal shift.

HTS-assay identifies eltrombopag, a previously documented viral entry inhibitor

From our screening, we have identified three new compounds that potentially inhibit the PPI of interest. However, we also found that eltrombopag is a potential TMPRSS2–SPIKE interaction inhibitor. Eltrombopag is an FDA-approved drug previously found to inhibit viral infection *in vitro* and bind to the SPIKE protein (Feng et al., 2020; Jeon et al., 2020). In this TR-FRET assay, eltrombopag had an IC_{50} of 20.6 ± 1.95 μM (Figure 8A and B) and generated a thermal shift of His-SPIKE-S2 with a ΔT_m of 1°C at 25 μM (Figure 8C). These results also suggest that eltrombopag may inhibit viral entry (Supplementary Figure S2), as previously reported.

Since eltrombopag was found via thermal shift assay to bind to His-SPIKE-S2, molecular docking of eltrombopag to SPIKE was done to investigate the potential binding site and mechanism of action. The analysis of the SPIKE surface revealed three putative small molecule binding sites (Figure 8D and E). Site 1 was located between R21, N121, L141, Q183, S247, G261, and Y265; Site 2 was found between T33, D290, L293, L296, K300, V608, and Y636; and Site 3 was surrounded by L48, K733, T778, K835, L849, N960, Y1007, and H1058. Interestingly, Site 2 occurs at the interface of TMPRSS2–SPIKE PPI, suggesting the potential to directly disrupt the PPI with a small molecule (Figure 8F and G).

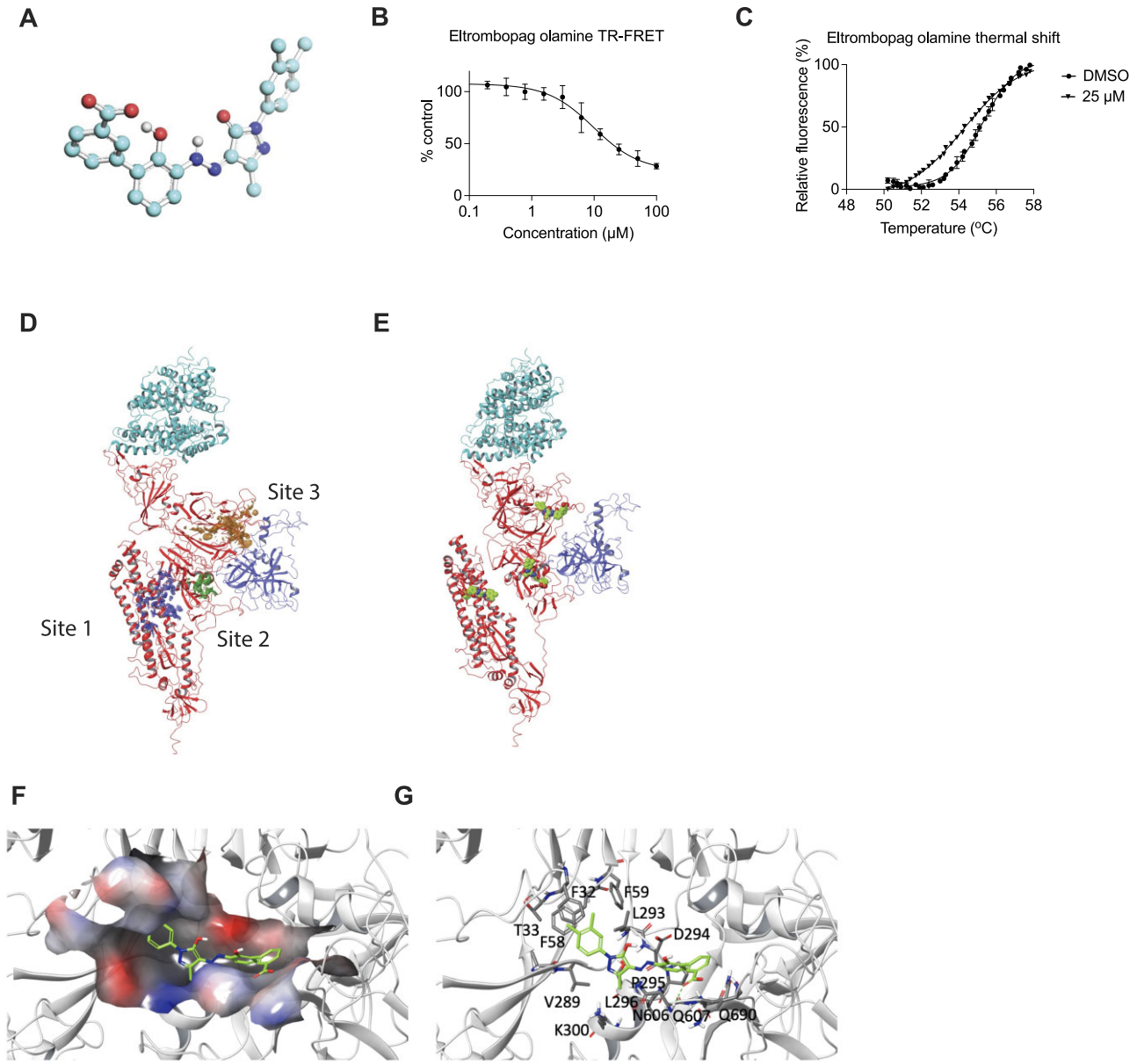

Figure 8 Evaluation of eltrombopag. (**A**) Predicted three-dimensional structure of eltrombopag generated in Maestro of the Schrodinger Small Molecule Drug Discovery suite of software. Light blue: carbon; dark blue: nitrogen; red: oxygen. (**B**) Eltrombopag in TR-FRET assay with an IC_{50} of ~20 μM using a nonlinear fit of inhibitor vs. response with a variable slope. Error bars represent the standard deviation of $n = 4$ values. (**C**) Eltrombopag with His-SPIKE-S2 in the SYPRO Orange thermal shift assay with a ΔT_m of 1°C compared to DMSO control at 25 μM when fit with the Boltzmann sigmoidal equation. (**D**) SiteMap identified three main binding sites of eltrombopag on SPIKE (red) when in complex with ACE2 (blue) and TMPRSS2 (purple). Site 2 is located at the interface of TMPRSS2 and SPIKE. (**E**) Eltrombopag can fit all three binding sites. (**F**) The molecular surface of the predicted eltrombopag binding site. Blue and red colors indicate positively and negatively charged atoms, respectively. (**G**) The predicted interactions of eltrombopag with SPIKE at the TMPRSS2–SPIKE PPI interface binding site.

Molecular docking of eltrombopag followed by MM-GBSA binding energy evaluation suggested that the compound can bind to Site 1, Site 2, and Site 3 with the estimated binding energy of −49.3, −59.5, and −76.3 kcal/mol, respectively. A detailed evaluation of ligand binding modes at each putative binding site revealed that eltrombopag could form three H-bonds with SPIKE K854, A831, and D830 at Site 1 with a total binding energy contribution of ΔG H-bond = −3.21 kcal/mol, one H-bond with N606 at Site 2 (ΔG H-bond = −1.68 kcal/mol), and three H-bonds with the backbone oxygen atom and the NH group of A260 (ΔG H-bond = −1.92 kcal/mol) at Site 3. However, the

lipophilic and van der Waals interactions contributed the most to eltrombopag binding to SPIKE, especially at Site 2 and Site 3 (Supplementary Table S2). Additionally, the electrostatic component was favorable for eltrombopag binding at Site 3 (ΔG Coulomb $= -44.15$ kcal/mol) and unfavorable at Site 1 (19.02 kcal/mol) and Site 2 (19.33 kcal/mol).

These data suggest that eltrombopag could act as an allosteric TMPRSS2–SPIKE PPI inhibitor and potentially serve as a direct PPI inhibitor at Site 2.

Discussion

The COVID-19 pandemic has wreaked havoc on the lives and businesses of millions of people across the world. Even though therapeutic development endeavors have been launched using a multitude of strategies, SARS-CoV-2 targeted therapies that have greater efficacy in certain populations and severely ill patients are urgently needed to improve clinical treatment outcomes (Zhao et al., 2022). Previous studies have demonstrated that TMPRSS2 cleaves and primes the SARS-CoV-2 SPIKE protein for viral attachment and membrane fusion (Hoffmann et al., 2020; Jackson et al., 2022). Our study shows the development and optimization of a 1536-well uHTS TR-FRET assay for the discovery of potential perturbagens that target the TMPRSS2–SPIKE interaction.

We first cloned SARS-CoV-2 SPIKE and TMPRSS2 into multiple expression vectors using the Gateway Cloning system. Constructs that expressed efficiently in HEK-293T cells were selected to confirm the interaction in an affinity chromatography assay. Then, lysates of cells overexpressing tagged TMPRSS2 and SPIKE proteins were used to develop the TR-FRET assay to provide a quantitative readout for the PPI. After testing multiple tag and TR-FRET antibody combinations, we selected the configuration that gave rise to an assay window and stability suitable for HTS, which was optimized for adaptation into the robot-enabled HTS platform. The assay was further miniaturized into the 1536-well format for uHTS, without compromising the signal, stability, or robustness of the assay.

To search for candidates for SARS-CoV-2 therapeutic interrogation and to demonstrate the power of our uHTS system, a pilot screening for small-molecule inhibitors that target the binding interface between SARS-CoV-2 SPIKE and TMPRSS2 was performed using a collection of bioactive libraries. We also developed a uHTS NanoBiT assay to orthogonally screen the top compounds from the TR-FRET assay for their activity against the TMPRSS2–SPIKE interaction.

Interestingly, eltrombopag, one of the hits from the pilot screen, was previously reported to bind to the SPIKE protein (Feng et al., 2020). Further confirming this, we demonstrated that eltrombopag binds to His-SPIKE-S2 using a thermal shift assay. This supports the premise that this TR-FRET assay can identify compounds that interact with the SPIKE or TMPRSS2 protein. Furthermore, eltrombopag is an FDA-approved compound used for the treatment of thrombocytopenia. As a consequence, the pharmacokinetic and toxicological profiles of eltrombopag in humans are already well documented, thereby representing a promising area of research for further drug development and providing the potential for expedited translation from bench to bedside.

Further analysis of the SPIKE structural model revealed three putative small molecule binding sites. The presence of multiple distinct ligand-binding sites on a protein surface is a common phenomenon. Thus, it is not surprising that the computational docking algorithms can fit eltrombopag to different SPIKE cavities. On the other hand, it is well known in the field that the agreement between calculated binding energy and experimentally determined binding affinity is limited, and computational determination of the most favorable small molecule binding site is a challenge.

SiteScores >0.8 indicated potential ligand-binding sites, whereas a SiteScore <0.8 indicated that the site is unlikely suitable for small molecule binding. The best SiteScores of 1.035 and 1.010 were obtained for Site 3 and Site 1, respectively. A lower SiteScore of 0.804 was found for Site 2, suggesting reduced ligandability of this site compared to Site 1 and Site 3. Meanwhile, this score is comparable with the SiteScores reported for other small-molecule PPI inhibitor binding sites (Shin et al., 2020). Alternatively, a detailed evaluation of ligand binding modes at each binding site revealed that we can rank the binding sites as Site 3 $>$ Site 2 $>$ Site 1, where Site 1 appears the least favorable for eltrombopag binding (ΔG bind $= -49.3$ kcal/mol).

Our experimental data show that eltrombopag disrupts the TMPRSS2–SPIKE complex. Furthermore, eltrombopag may bind at the interface of two proteins, and the binding of eltrombopag at Site 2 is most consistent with the experimental data. However, we cannot exclude the possibility of allosteric regulation of TMPRSS2–SPIKE by eltrombopag through Site 3. Future detailed site-directed mutagenesis, biophysical, and biostructural experiments are required to precisely identify the binding mode of eltrombopag at the SPIKE surface.

To the best of our knowledge, this is the first study of PPI inhibitors of the TMPRSS2–SARS-CoV-2 SPIKE interaction. All hits from this screening need to be confirmed as inhibitors of the TMPRSS2–SPIKE interaction via orthogonal assays, such as affinity chromatography or biophysical experiments, to disrupt the TMPRSS2–SPIKE interaction. As this is a cell lysate-based assay, additional live-cell and virus-based models will be important for the validation to ensure that the compounds disrupt the PPIs in their native environment and effectively prevent viral infection. A diversity of chemical libraries will also be included in future endeavors to identify novel small-molecule probes for chemical biology investigations of the TMPRSS2–SPIKE interaction, as well as novel therapeutic strategies to target this interaction.

In summary, with demonstrated robust assay performance, our uHTS TR-FRET assay can enable sensitive and cost-efficient identification of candidate compounds from the vast chemical space to perturb the TMPRSS2–SPIKE interaction utilized by SARS-CoV-2 to enter into human cells and cause disease.

Materials and methods

Cell lines and culture conditions

HEK-293T cell line was obtained from the American Type Culture Collection (ATCC, CRL-3216). The cells were cultured in Dulbecco's modified Eagle's medium (Corning, 10-013-CV), supplemented with 10% fetal bovine serum (Sigma, F0926), and 1% penicillin–streptomycin solution (Corning, 30-002-CI) at 37°C in humidified conditions with 5% CO_2.

PCR and cloning

All plasmids for the expression of proteins with His, FLAG, VF, and GST tags were cloned using the Gateway Cloning system (Invitrogen) as described previously (Li et al., 2017). The DNA was purified using the ZymoPURE Plasmid Maxiprep Kit (Zymo Research, D4203).

The SPIKE coding sequence was synthesized from GeneArt (Thermo Fisher Scientific) based on the viral sequence isolated from Wuhan (NCBI reference sequence: NC_045512.2) and modified to be compatible with mammalian expression. Sequences were verified via sequencing and restriction enzyme digest. TMPRSS2 entry clone was purchased from DNASU (Clone ID: HsCD00513790).

Transfection

HEK-293T cells were transfected using 1 mg/ml polyethyleneimine or FuGENE HD (Promega, E2312) in a ratio of 3 μl to 1 μg DNA and incubated for 48 h.

GST pulldown

Constructs for GST-TMPRSS2 and SPIKE-VF were co-transfected into HEK-293T cells, and cells were collected after 48 h of transfection. Cells were lysed via vortexing and 5-sec sonication using 200 μl of 1% NP-40 lysis buffer (20 mM Tris–HCl, 137 mM NaCl, 2 mM EDTA, 5% glycerol, and 1% NP-40) with 1:100 protease inhibitor cocktail (Sigma, P8340), PIC3 (Sigma, P0044), and PIC2 (Sigma, P5726). Glutathione Sepharose 4B beads (GE, 17-0756-05) were pre-washed and 20 μl were added to tubes with 170 μl of lysate. Beads were rotated for 3 h at 4°C, and then washed three times with lysis buffer. After liquid was removed, 30 μl of 2× Laemmli buffer (Bio-Rad, 1610737) was added per tube, and samples were boiled for 10 min to be used in western blotting.

Western blotting

Samples were run on a 10% sodium dodecyl sulfate–polyacrylamide gel and transferred to nitrocellulose membranes at 100 V for 2.5–3 h at 4°C. Membranes were blocked in 5% nonfat dry milk in TBST buffer (20 mM Tris–HCl, 150 mM NaCl, and 0.05% Tween 20) for 30 min to 1 h, and primary antibodies were added for overnight incubation at 4°C. After washing the membranes three times with TBST buffer, the secondary antibody was added for 1–1.5 h incubation at room temperature. Then, the membranes were washed three times with TBST buffer. Thermo Scientific SuperSignal West Pico PLUS Chemiluminescent Substrate (Thermo, 34580) was used to develop membranes. The western blot imaging was performed using the ChemiDoc Imaging System (Bio-Rad).

Antibodies

Tb cryptate-labeled anti-GST antibody (anti-GST-Tb, 61GSTTLB), D2-labeled anti-FLAG M2 antibody (anti-FLAG-D2, 61FG2DLB), D2-labeled anti-GST antibody (anti-GST-D2, 61GSTDLB), Tb cryptate-labeled anti-FLAG M2 antibody (anti-FLAG-Tb, 61FG2TLB), Tb cryptate-labeled anti-His antibody (anti-His-Tb, 61HisTLB), and D2-labeled anti-His antibody (anti-His-D2, 61HisDLB) were purchased from Cisbio Bioassays. Monoclonal anti-FLAG M2-Peroxidase antibody (A8592), anti-GST-Peroxidase antibody (A7340), anti-ACTIN antibody (A5441), and anti-His antibody (SAB1306085) were purchased from Sigma. Peroxidase AffiniPure goat anti-rabbit IgG (H + L) secondary antibody (111-035-003) and Peroxidase AffiniPure goat anti-mouse IgG (H + L) secondary antibody (115-035-003) were purchased from Jackson ImmunoResearch. Anti-TMPRSS2 antibody (ab92323) was purchased from Abcam.

TR-FRET assay development

Various combinations of constructs were co-transfected into HEK-293T cells, and cells were collected after 48 h of transfection. Cells were lysed via vortexing and 5-sec sonication using 1% NP-40 lysis buffer. Lysate (15 μl) was serially diluted in 15 μl of FRET buffer (20 mM Tris–HCl, pH 7.0, 50 mM NaCl, and 0.01% NP-40) in a 384-well plate (Corning, 3573), and 15 μl of antibody mix (1:1000 anti-FLAG-Tb and 1:500 anti-His-D2, Cisbio) was added for a total of 30 μl per well of reaction. The plate was spun down, stored at 4°C, and read after 2 h using the BMG LABTECH PHERAstar FSX plate reader. The following settings were used for the Tb/D2 pairs: excitation at 337 nm (laser); emission 1 at 615 nm; emission 2 at 665 nm; time delay for 50 μs. The TR-FRET signal is expressed as the FRET ratio 665 nm/615 nm $\times$ 10^4.

TR-FRET assay optimization

Lysate of cells expressing His-TMPRSS2 and SPIKE-FLAG, which gave rise to the robust signal from the above assay development, was tested and evaluated for HTS assay performance. The lysate dilution that produced an S/B >10 within the dynamic range was chosen for DMSO and temporal stability assays. To test stability in DMSO, lysate was diluted with antibodies in FRET buffer and added to a 384-well plate with DMSO at various concentrations. Plates were spun down, stored at 4°C, and read after 2 h. For temporal stability, lysates were diluted with antibodies and plated in a 384-well plate. Plates were spun down, stored at 4°C, and read at 2, 6, 24, and 48 h.

Miniaturization of TR-FRET assay into 1536-well uHTS format

Lysate dilution with an S/B >10 within the dynamic range in a 384-well plate was chosen for the assay. Diluted lysate and antibodies were dispensed into both 384- and 1536-well black solid-bottom plates (Corning, 3724), using the MultiDrop Combi dispenser (Thermo, 5840320) to dispense 30 μl/well into 384-well plates and 5 μl/well into 1536-well plates, respectively.

Pilot screening using uHTS TR-FRET assay

Lysate dilution was chosen by testing the TR-FRET signal of serially diluted lysate in a 384-well plate. Diluted lysate (5–15 μg/ml) was dispensed into 1536-well plates (5 μl/well) as stated above. The uHTS assays were performed with the in-house LOPAC (Sigma, LO1280-1KT) and Emory Enriched Bioactive Library chemical libraries (Mo et al., 2017). The library compounds were dissolved in DMSO, and 0.1 μl was added to each well in quadruplicate using a pin tool integrated with Beckman NX (Beckman Coulter) or the Beckman i5 automated workstation (Beckman Coulter). DMSO served as vehicle control. After centrifugation at 200× *g* for 3 min and incubation for at least 1 h, TR-FRET signal was measured using a BMG LABTECH PHERAstar FSX plate reader.

Screening data were analyzed using the CambridgeSoft Bioassay software or GraphPad Prism. The performance of the assay for each screening plate was evaluated by Z-factor and S/B ratio, which were calculated using the following equations:

$$\text{Z-factor} = 1 - (3 \times \text{SD}_{\text{DMSO}} + 3 \times \text{SD}_{\text{blank}})/(F_{\text{DMSO}} - F_{\text{blank}}),$$
$$\text{S/B} = F_{\text{DMSO}}/F_{\text{blank}},$$

where SD_{DMSO} and SD_{blank} are the standard deviations, and F_{DMSO} and F_{blank} are the corresponding average TR-FRET signals for the wells with DMSO control and buffer background, respectively. A Z-factor between 0.5 and 1.0 indicates that the assay is robust for HTS (Zhang et al., 1999). The compound effect was determined by the percent of TR-FRET signal of the compound to the control signal (% control), based on the control per plate, and calculated using the following equation:

$$\%\,\text{control} = \left(F_{\text{compound}} - F_{\text{blank}}\right) / \left(F_{\text{DMSO}} - F_{\text{blank}}\right) \times 100\%.$$

NanoBiT assay

SmBiT and LgBiT fused at the N- or C-terminal region of TMPRSS2 and SPIKE were cloned with Gateway Cloning. HEK-293T cells were transfected with various combinations of the constructs using 3 μl of Fugene to 1 μg of DNA. Cells were collected after 18–24 h and replated in a white 1536-well plate (Corning, 3727) with the MultiDrop Combi dispenser and cultured overnight. Nanoluciferase substrate (Promega, N2012) was added to cells at a final dilution of 100× with the MultiDrop Combi dispenser. Plates were spun down at 200× *g* for 3 min and shaken for 10–15 sec. Luminescence signal was read with the BMG LABTECH PHERAstar FSX plate reader. For compound testing, a total of 3500 HEK-293T cells expressing SmBiT-TMPRSS2 and SPIKE-LgBiT were replaced into each well of a 1536-well plate in 5 μl growth medium. After overnight incubation, cells in each well were treated with 0.1 μl compound (stored at 1 mM) for 5 h. The luciferase signal was read by adding the nanoluciferase substrate.

Reordered compounds

Closantel (HY-17596), CAPE (HY-N024), and AG-490 (HY-12000) were ordered from MedChemExpress. GW4064 (S2782), gossypol acetate (S2303), and eltrombopag olamine (S2229) were ordered from Selleckchem. Verteporfin (B1583-5) was ordered from BioVision.

Thermal shift assay

SYPRO Orange (Thermo, S6650) was added at a final dilution of 4× to 20 μl of 200 μg/ml His-SPIKE-S2 (Acrobio, S2N-C52H5) in PBS. One microliter of compound was added for a final concentration of 25 μM to protein sample in a PCR plate in duplicate (Midsci, PR-PCR3196). A thermocycler (Eppendorf Realplex Epgradient S) was used to heat samples up to 80°C over 30 min.

Computational modeling

A homology model of SPIKE protein was built using the Schrodinger Prime software based on the Cryo-EM structures of the human (PDB ID: 7DF4) and Pangolin coronavirus (PDB ID: 7CN8) SPIKE proteins. Each chain of SPIKE protein was modeled individually. Then, the individual chains were superimposed with the 7DF4 SPIKE structure to form the SPIKE trimer. The energy of the resulting model was minimized using the Schrodinger MacroModel program with the Polak–Ribier conjugate gradient minimization method, the OPLS4 force field, and the coverage threshold of 0.05. The unconstrained protein–protein docking was conducted between SPIKE as a receptor and TMPRSS2 (PDB ID: 7MEQ) as a ligand. A total of 70000 ligand rotations were probed. The small molecule binding sites at SPIKE proteins were identified using the Schrodinger SiteMap tool (Shin et al., 2020). Small molecule docking was performed using the Schrodinger Glide software (Friesner et al., 2006) in the standard precision mode with the default settings.

Supplementary material

Supplementary material is available at *Journal of Molecular Cell Biology* online.

Funding

This research was supported in part by the Emory School of Medicine COVID Catalyst-I3 award (H.F. and S.G.S.), the NCI Emory Lung Cancer SPORE (P50CA217691) Career Enhancement Program (A.A.I.), Emory Initiative on Biological Discovery through Chemical Innovation (A.A.I.), and R01AI167356 (S.G.S.).

Conflict of interest: none declared.

Author contributions: D.C.: investigation, conceptualization, methodology, writing, and editing; Q.N.: conceptualization, methodology, investigation, and editing; Y.D.: formal analysis and methodology; M.Q.: investigation; A.A.I.: investigation, visualization, and writing; K.Q.: validation; E.M.: visualization and editing; D.F.: validation; X.M.: conceptualization and editing; S.G.S.: part of I3 funding and editing; and H.F.: conceptualization, funding acquisition, supervision, writing review, and editing.

References

Dixon, A.S., Schwinn, M.K., Hall, M.P., et al. (2016). NanoLuc complementation reporter optimized for accurate measurement of protein interactions in cells. ACS Chem. Biol. *11*, 400–408.

Feng, S., Luan, X., Wang, Y., et al. (2020). Eltrombopag is a potential target for drug intervention in SARS-CoV-2 spike protein. Infect. Genet. Evol. *85*, 104419.

Friesner, R.A., Murphy, R.B., Repasky, M.P., et al. (2006). Extra precision glide: docking and scoring incorporating a model of hydrophobic enclosure for protein–ligand complexes. J. Med. Chem. *49*, 6177–6196.

Gupta, A., Gonzalez-Rojas, Y., Juarez, E., et al. (2022). Effect of sotrovimab on hospitalization or death among high-risk patients with mild to moderate COVID-19: a randomized clinical trial. JAMA *327*, 1236–1246.

Hammond, J., Leister-Tebbe, H., Gardner, A., et al. (2022). Oral nirmatrelvir for high-risk, nonhospitalized adults with COVID-19. N. Engl. J. Med. *386*, 1397–1408.

Hoffmann, M., Hofmann-Winkler, H., Smith, J.C., et al. (2021). Camostat mesylate inhibits SARS-CoV-2 activation by TMPRSS2-related proteases and its metabolite GBPA exerts antiviral activity. EBioMedicine *65*, 103255–103255.

Hoffmann, M., Kleine-Weber, H., Schroeder, S., et al. (2020). SARS-CoV-2 cell entry depends on ACE2 and TMPRSS2 and is blocked by a clinically proven protease inhibitor. Cell *181*, 271–280.e8.

Jackson, C.B., Farzan, M., Chen, B., et al. (2022). Mechanisms of SARS-CoV-2 entry into cells. Nat. Rev. Mol. Cell Biol. *23*, 3–20.

Jayk Bernal, A., Gomes da Silva, M.M., Musungaie, D.B., et al. (2022). Molnupiravir for oral treatment of COVID-19 in nonhospitalized patients. N. Engl. J. Med. *386*, 509–520.

Jeon, S., Ko, M., Lee, J., et al. (2020). Identification of antiviral drug candidates against SARS-CoV-2 from FDA-approved drugs. Antimicrob. Agents Chemother. *64*, e00819–e00820.

Klostermeier, D., and Millar, D.P. (2002). Time-resolved fluorescence resonance energy transfer: a versatile tool for the analysis of nucleic acids. Biopolymers *61*, 159–179.

Li, Z., Ivanov, A.A., Su, R., et al. (2017). The OncoPPi network of cancer-focused protein–protein interactions to inform biological insights and therapeutic strategies. Nat. Commun. *8*, 14356.

Malik, J.A., Mulla, A.H., Farooqi, T., et al. (2021). Targets and strategies for vaccine development against SARS-CoV-2. Biomed. Pharmacother. *137*, 111254.

Mo, X., Qi, Q., Ivanov, A.A., et al. (2017). AKT1, LKB1, and YAP1 revealed as MYC interactors with NanoLuc-based protein-fragment complementation assay. Mol. Pharmacol. *91*, 339–347.

Mo, X., Tang, C., Niu, Q., et al. (2019). HTiP: high-throughput immunomodulator phenotypic screening platform to reveal IAP antagonists as anti-cancer immune enhancers. Cell Chem. Biol. *26*, 331–339.e3.

Papa, G., Mallery, D.L., Albecka, A., et al. (2021). Furin cleavage of SARS-CoV-2 spike promotes but is not essential for infection and cell–cell fusion. PLoS Pathog. *17*, e1009246.

Shin, W.-H., Kumazawa, K., Imai, K., et al. (2020). Current challenges and opportunities in designing protein–protein interaction targeted drugs. Adv. Appl. Bioinform. Chem. *13*, 11–25.

Tang, C., Mo, X., Niu, Q., et al. (2021). Hypomorph mutation-directed small-molecule protein–protein interaction inducers to restore mutant SMAD4-suppressed TGF-β signaling. Cell Chem. Biol. *28*, 636–647.e5.

Xiong, J., Pecchi, V.G., Qui, M., et al. (2018). Development of a time-resolved fluorescence resonance energy transfer ultrahigh-throughput screening assay for targeting the NSD3 and MYC interaction. Assay Drug Dev. Technol. *16*, 96–106.

Yang, X., Yu, Y., Xu, J., et al. (2020). Clinical course and outcomes of critically ill patients with SARS-CoV-2 pneumonia in Wuhan, China: a single-centered, retrospective, observational study. Lancet Respir. Med. *8*, 475–481.

Zhang, J.-H., Chung, T.D., and Oldenburg, K.R. (1999). A simple statistical parameter for use in evaluation and validation of high throughput screening assays. J. Biomol. Screen. *4*, 67–73.

Zhao, L., Li, S., and Zhong, W. (2022). Mechanism of action of small-molecule agents in ongoing clinical trials for SARS-CoV-2: a review. Front. Pharmacol. *13*, 840639.